ACS Macro Letters

pubs.acs.org/macroletters Letter

Network Topology and Percolation in Model Covalent Adaptable Networks

Benjamin R. Hafner, Subhadeep Pal, Broderick Lewis, Sinan Keten, and Kenneth R. Shull*

Cite This: ACS Macro Lett. 2024, 13, 1545−1550 Read Online

ACCESS | Metrics & More | Article Recommendations | Supporting Information

ABSTRACT: Incorporating dynamic covalent linkages into thermosets can endow previously unrecyclable materials with new functionality and reprocessing options. Recent work has shown that the properties of the resulting covalent adaptable networks (CANs) are highly dependent on network topology, specifically the phenomenon of percolation, when permanent linkages form a connected skeleton that spans the material. Here, we use a model glassy disulfide based CAN to assess the merits of mean-field percolation theory as a tool to describe the network topology of CANs. After challenging the theory with both experimental data and a coarse-grained molecular dynamics simulation, we find that the mean-field approach is surprisingly accurate, despite its simplifying assumptions. The theory is particularly well suited to the unique context of mixed-composition CANs and provides practical guidance on how to design for reprocessability.

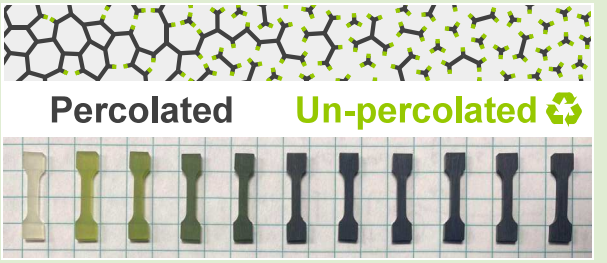

Covalent adaptable networks (CANs) retain the outstanding mechanical properties and solvent resistance of conventional covalently cross-linked thermosets, but under the right stimulus, their dynamic covalent linkages can exchange, allowing the network to rearrange to give a material with thermoplastic properties. The possibility of combining the performance of thermosets with the processability and recyclability of thermoplastics has attracted significant research in the past decade, and numerous dynamic chemistries have been explored.[1] But regardless of the specific chemistry, from a topological perspective, each network linkage in a CAN can often be simplified to a binary classification: "dynamic" if it can exchange or "permanent" if it cannot. Mixed-composition CANs, also known as "partial vitrimers," incorporate a mix of both permanent and dynamic linkages to achieve different balances between creep resistance, ease of reprocessing, cost, or other factors.[2−4] Depending on the permanent to dynamic ratio, two distinct regimes emerge:

1. **The percolated regime.** If too many linkages are permanent, they will connect up into a skeleton that percolates through the network and holds fast no matter how much the dynamic linkages exchange. This percolated skeleton prevents complete stress relaxation and resists the large deformations required for thermoforming and recycling.
2. **The unpercolated regime.** On the other hand, when more than a critical fraction of linkages are dynamic, no percolated skeleton forms. In this case small clusters of the network may still be held together by permanent linkages, but these clusters are finite in size. Furthermore, the clusters can move past each other as the dynamic linkages exchange, allowing the material to be reshaped.

Given the decisive role of percolation in reprocessability for CANs, there is a practical need for a theory that accurately predicts the percolation threshold, where the transition between these two regimes occurs. One promising candidate is the mean-field theory of percolation, first laid out by Flory in 1941,[5,6] refined by Stockmayer in 1943,[7] and notably rederived by Miller and Macosko in 1976.[8,9] The theory was originally developed to describe the onset of gelation during step-growth polymerization, but the formation of a permanent skeleton in a mixed-composition CAN is governed by the same principles of percolation. In the past few years, several authors have made use of this gelation analogy to apply mean-field percolation theory to CANs and have reported some encouraging qualitative agreement with experimental results[3,4,10,11]

In addition to the percolation threshold, the mean-field approach can also predict other topological parameters like the concentration of elastically effective network strands in the percolated skeleton (relevant for residual stress in the percolated regime) and the distribution of finite cluster sizes (relevant for viscosity in the unpercolated regime). The theory's ability to predict these practically relevant parameters with just a few simple equations makes it especially enticing to the CAN research community. However, this utility comes at the cost of two simplifying assumptions:

Received: August 2, 2024
Revised: October 7, 2024
Accepted: October 8, 2024

https://doi.org/10.1021/acsmacrolett.4c00523
ACS Macro Lett. 2024, 13, 1545−1550

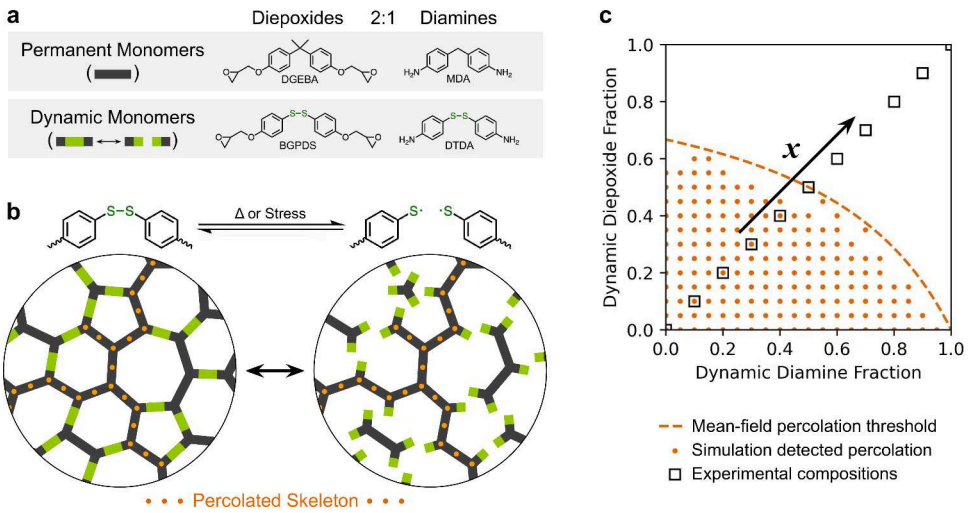

Figure 1. System overview showing (a) monomer structures, (b) schematic of percolation, and (c) a two-dimensional map of the composition space.

1. **Perfect Cure.** During cure, each monomer is equally likely to bond to another dynamic monomer as to another permanent monomer, and all monomers fully react.
2. **No loops.** Finite permanent clusters contain no loops. (Loops are allowed in the percolated skeleton.)

While the mean-field theory can be modified to account for incomplete cure and unequal reactivities (see Supporting Information (SI) section 6), the no-loops assumption is more difficult to relax. To account for loops, one must turn to critical percolation theory, which relies on scaling arguments and large simulations to estimate critical exponents—an approach that provides valuable insight in the limit as clusters become very large or very close to the percolation threshold, but is less useful in predicting concrete values of practical parameters.[12]

Given this context, it is unclear whether or not mean-field percolation theory is adequate to model the network topology of mixed-composition CANs. The theory is simple and easy to apply, but is it accurate enough to effectively guide design for reprocessability, or do its simplifying assumptions defeat its utility? The work described here challenges the theory with experimental and simulation data for a model CAN system. We probe network topology experimentally with mass spectrometry, gel fraction measurements, and creep tests, as well as computationally with coarse-grained molecular dynamics simulations. We then compare the results of experiment, simulation, and theory side by side. We aim both to assess the merits of the mean-field approach in the context of CANs, and to emphasize the practical implications of percolation on reprocessability.

The model CAN used here incorporates dynamic aromatic disulfide bonds into a tightly cross-linked epoxy-amine thermoset. At elevated temperatures, a small fraction of disulfide bonds spontaneously break, forming stable sulfur-based radicals which then exchange with other disulfide bonds.[13,14] As this radical-mediated exchange continuously rearranges the network, the material can be thermoformed, healed, or reprocessed like a thermoplastic.[15] In addition to catalyst-free reprocessability, the system also boasts excellent strength and toughness (due in part to sacrificial disulfide cleavage under high strain as an energy dissipation mechanism),[16] vibrant mechanochromism,[17] and a high glass transition temperature (T_g = 125−190 °C)[18] that stands out against a landscape of CANs dominated by low-T_g elastomers (see SI section 2 for further discussion of the glass transition and mechanical properties).

To produce networks with a mix of permanent and dynamic linkages, conventional "permanent" monomers diglycidyl ether of bisphenol A (DGEBA) and 4,4′-methylenedianiline (MDA) were combined at various ratios with structurally similar disulfide-containing "dynamic" monomers bis(4-glycidyloxyphenyl) disulfide (BGPDS) and 4,4′-dithiodianiline (DTDA) (first reported in 2016 and 1990, respectively[19,20]). While the total ratio of epoxide groups to amine groups was held at 2:1 to maintain stoichiometric balance, the fraction of dynamic monomers was varied. Since the fraction of dynamic diepoxides (BGPDS vs DGEBA) and the fraction of dynamic diamines (DTDA vs MDA) can each be varied independently, the available composition space is represented as a two-dimensional map in Figure 1c.

Percolation occurs in the lower left portion of the composition map, when too few monomers are dynamic. The mean-field prediction for the boundary of this percolated regime is marked by the dashed curve in Figure 1c (see SI section 5 for a derivation the curve's equation: $(1-x_{\text{epoxide}})\ (3-2x_{\text{amine}}) = 1$). As a preliminary test of this prediction, the composition space was sampled at 5% increments in both dimensions and each point was tested for percolation with a coarse-grained molecular dynamics (CG-MD) model, similar to that described by Pal et al.[21] and Giuntoli et al.[22] By representing the diepoxide and diamine monomers as short chains of simple beads, the model requires orders of magnitude less computational resources than comparable all-atomistic approaches. An ensemble of 2000 diepoxides and 1000 diamines was generated in LAMMPS and cross-linked with Polymatic[23] to ∼97% cure (SI section 8). After equilibration at 300 K and 1 atm, all dynamic monomers were split in half, cleaving the network into permanent clusters. A MATLAB program recorded the distribution of cluster sizes and tested for "wrap-around" clusters, which extend past the periodic boundary condition and then wrap around to connect back to themselves, a tell-tale sign of percolation.[24] In Figure 1c, compositions where a wrap-around cluster was detected are marked with orange dots. The threshold of this simulation-based litmus test appears to fall slightly below the mean-field prediction (dashed curve). Encouragingly, this systematic discrepancy due to the presence of loops and incomplete cure (SI section 6) is only minor, and the general shape matches well.

https://doi.org/10.1021/acsmacrolett.4c00523
ACS Macro Lett. 2024, 13, 1545−1550

Next, in order to demonstrate the practical impact of percolation on reprocessability, physical samples were prepared and tested for thermomechanical and chemical recyclability. Unfortunately, it would be prohibitively time-consuming to conduct an experimental survey of the entire two-dimensional composition space. Instead, we concentrate only on the diagonal shown in Figure 1c, which spans from fully permanent (DGEBA/MDA) to fully dynamic (BGPDS/DTDA). We use the parameter x as a shorthand for both the mole fraction of dynamic diepoxides and the mole fraction of dynamic diamines, which are equal on the diagonal. The 11 compositions prepared range from $x = 0$ to $x = 1$ by increments of 0.1.

Qualitative high temperature creep was used as a proxy test for thermomechanical recyclability. At high temperatures, the dynamic linkages should freely exchange, enabling creep or even flow and allowing the material to be formed into a new shape for reuse. Percolation, however, was found to prevent flow and suppresses creep even at high temperatures (although some transient relaxation is still expected as stress is transferred to the skeleton). When dog-bone samples of each composition were heated to 220 °C (well above T_g) under ∼0.3 MPa stress for 3 h, a clear threshold was observed: No long-term creep occurred when $x < 0.5$, but there was extensive flow when $x \geqslant 0.5$ (see Figure 2).

For chemical recycling (which may be more appropriate for composites with valuable fillers), solubility was used as a proxy test. In the presence of a reducing agent, the disulfide bonds can be cleaved into thiols, breaking up the network into small soluble molecules.[15,19,25] To test this recycling strategy, a small (∼40 mg) sample of each composition was submerged in 1 mL of dimethylformamide (DMF) solvent with 0.5 M dithiothreitol (DTT) reducing agent at 85 °C for 3 days. Again, a stark threshold emerged: above $x = 0.5$ all samples fully dissolved, whereas below $x = 0.5$ they appeared swollen but insoluble, due to the formation of a percolated skeleton. As with the creep test, the onset of percolation inhibited recyclability.

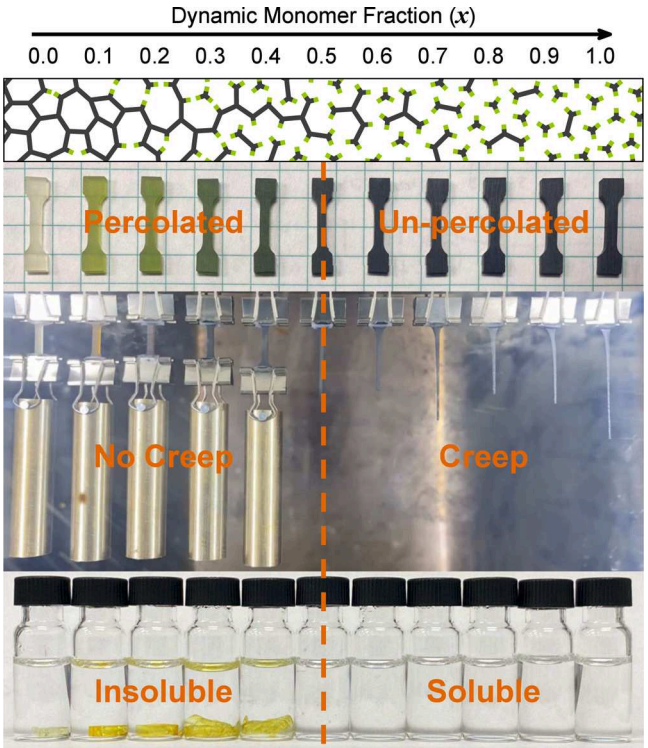

Figure 2. A visual demonstration contrasting the percolated and unpercolated regimes. Because the samples on the left contain a permanent percolated skeleton, they resisted creep even after 3 h at 220 °C and remained insoluble even after 3 days in DMF with 0.5 M DTT reducing agent to break all disulfide bonds. The unpercolated samples on the right, in contrast, flow at high temperatures and are soluble in DMF/DTT, opening the door to both thermomechanical and chemical recycling. A time-lapse video of the creep experiment is included in the Supporting Information.

The $x = 0.5$ threshold observed in both creep and solubility agrees exactly with the mean-field prediction: in a network where every linkage has probability x of being dynamic and linkages meet at junctions of functionality f, the mean-field percolation threshold is given by[5]

$$x_{\text{perc}} = \frac{f-2}{f-1} \tag{1}$$

In this case, three linkages meet at every junction (two epoxides and one amine) so $f = 3$, and $x_{\text{perc}} = 0.5$, as expected. Note that no distinction was required between diepoxide linkages and diamine linkages, because from a topological perspective, each linkage is dynamic with probability x and permanent with probability $1-x$, whether a diepoxide or a diamine. For compositions not on the diagonal shown in Figure 1c, this assumption fails, and a more detailed approach is required (SI section 5).

The mean-field theory's agreement with both creep and solubility experiments is promising. However, while these experimental results are visually striking, they are somewhat lacking in precision. At best, the percolation threshold was only determined to the nearest 10%. One could proceed by testing finer and finer compositional increments (e.g., $x = 0.45, 0.55$), but it would quickly become difficult to distinguish slow creep from long transient relaxation, or sluggish dissolution from insolubility. To circumvent this problem, more sophisticated testing was required. Instead of simply classifying each composition as percolated or unpercolated, we measured the mass fraction of the percolated component and the mass fraction of each finite cluster size, all of which are also predicted by the mean-field theory. This approach enables a more comprehensive and more precise assessment of the theory's predictions, which we compare against both simulation and experiment.

The mean-field theory predicts the following mass breakdown when each linkage is dynamic with probability x and three linkages meet at each junction ($f = 3$)

$$w_1 = x^3$$

$$w_2 = 3x^4(1-x)$$

$$w_3 = 9x^5(1-x)^2$$

$$w_4 = 28x^6(1-x)^3$$

$$w_n = \frac{3(2n)!}{(n-1)!(n+2)!}x^{n+2}(1-x)^{n-1}$$

$$w_\infty = \begin{cases} 1-(x/(1-x))^3 & x < 0.5 \\ 0 & x > 0.5 \end{cases}$$

where w_n is the mass fraction of clusters with n junctions and w_∞ is the mass fraction of the percolated network. These results are largely analogous to those previously reported in the context of gelation, but we have included a full derivation from first-

https://doi.org/10.1021/acsmacrolett.4c00523
ACS Macro Lett. 2024, 13, 1545−1550

principles specific to the context of mixed-composition CANs (SI section 3), as well as a generalization beyond $f = 3$ (SI section 4). The SI also contains useful formulas for the weight-average molecular weight (M_w) of finite clusters, which diverges at the percolation threshold, and the elastically effective cross-link density (ν) of the percolated network, which goes to zero at the percolation threshold (SI section 3).

Before proceeding, it is worth calling out the assumptions implicit in the above predictions. Each monomer's probability of being dynamic is assumed to be independent of its surroundings (dynamic monomers do not phase separate, for example). And, critically, the finite clusters are assumed to be tree-like (no loops). Finally, the above distribution assumes that every junction has the same mass. This last assumption can be relaxed to account for the difference between dynamic and permanent monomer masses, but the effect is small (SI section 7).

To measure the network's mass breakdown experimentally, two techniques were used. First, the percolated mass fraction, w_∞, was measured by simply weighing the insoluble remnants from the dissolution experiments, after they were soaked in a fresh DMF/DTT solution, rinsed in acetone, and dried under vacuum. The measured insoluble mass fractions (open orange circles in Figure 3) were systematically higher than the mean-field predictions (orange line in Figure 3), but still followed a similar trend. Surprisingly, several of the insoluble remnants were even heavier than their original samples, suggesting unphysical insoluble mass fractions greater than one. The systematic mass gain may be due to residual DMF, either permanently incorporated into the network or not fully evaporated, despite drying for 7 days at 85 °C.

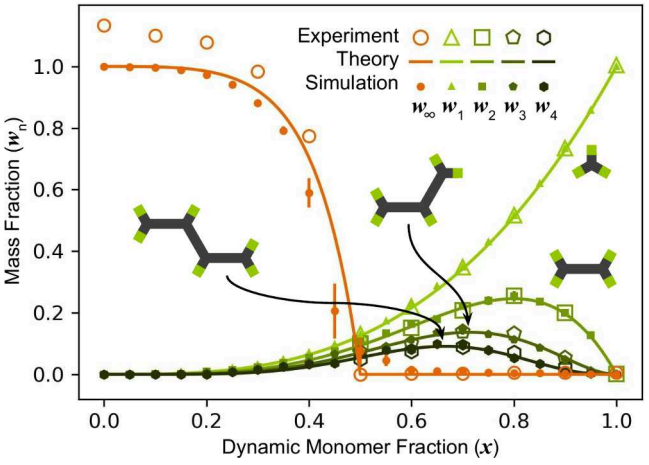

Figure 3. Comparison of experimental and simulated results with mean-field theory predictions. The finite cluster mass fractions (w_1, w_2, w_3, w_4) were experimentally determined via mass spectrometry, while the percolated mass fraction (w_∞) was determined by gel fraction. A coarse-grained molecular dynamics model with 2000 diamines and 1000 diepoxides was used for the simulation. All solid symbols have error bars representing the standard deviation over 5 trials, though most are smaller than the symbol size.

The mass spectra provided only relative amounts of each cluster size, so each spectrum was normalized by scaling the first cluster peak to match the theoretical prediction, w_1 (thus, the open triangles in Figure 3 perfectly match the predicted curve). Furthermore, the technique is not equally sensitive to different cluster sizes, necessitating 3 fitting parameters to scale the results for w_2, w_3, and w_4, respectively. For example, the w_2 values (open squares in Figure 3) were uniformly scaled down by 0.65. Thus, the absolute amount of each cluster size is arbitrary, it is only the trends across x-values that are meaningful (SI section 10).

To provide another point of comparison, the same values (w_1, w_2, w_3, w_4, and w_∞) were also measured in the coarse-grained molecular dynamics (CG-MD) model. Thanks to the model's computational efficiency, more compositions could be explored, and each composition was simulated five times, yielding averages and standard deviations for each mass fraction.

The mean-field predictions, experimental observations, and simulated results are all plotted together in Figure 3. Overall, the agreement between theory, experiment, and simulation is quite strong, suggesting that the experimental and simulated systems are nearly ideal, fully cured networks. In fact, the accuracy of the mean-field predictions is somewhat surprising, given its neglect of network loops, which are inevitable in large clusters. Typically, this neglect leads to inaccurate predictions, which necessitate the application of critical percolation theory instead. This issue is particularly relevant for systems with small, densely cross-linked monomers that are prone to loops.[26] Interestingly, the mean-field predictions here do not seem to suffer from this inaccuracy, but it is still worth briefly discussing critical percolation theory and its implications for context.

Critical percolation theory was developed in the 1970s and '80s primarily to predict asymptotic behavior near the percolation threshold, where clusters grow so large that they must contain many loops, clearly violating the mean-field assumptions. While critical percolation theory does not predict absolute mass fractions, it does predict critical exponents near the percolation threshold, which differ significantly from those predicted by mean field theory. For this reason, one might expect the experimental and simulated results to substantially deviate from the mean-field prediction near the percolation threshold, but Figure 3 shows no such substantial deviation. The simulated percolated mass fraction w_∞ (solid orange circles) does show a slight deviation—it appears somewhat rounded near the percolation threshold—but this rounding is merely an artifact of the simulation's finite size (SI section 9). Neither mean-field nor critical percolation theory predicts any rounding at percolation: in the mean-field model, w_∞ shows an instantaneous slope change from −12 to 0 at $x = x_{perc}$, and in the critical percolation model the slope actually approaches infinity (w_∞ goes as $(x_{perc}-x)^\beta$ with $\beta < 1$) before instantaneously transitioning to 0 at $x = x_{perc}$.[12] Within the resolution of the simulations and experiments conducted, there is no evidence of any significant deviation from mean-field theory, and no evidence that critical percolation theory would provide a better description of the data.

So, why is the mean-field theory so accurate here, when conventional wisdom says it should fail for systems like this with small densely cross-linked monomers? We propose a 2-fold explanation. First, the monomers are stiff, so they resist the bending required to form small loops (see SI section 11 for a discussion of looping probabilities). Instead, they tend to branch straight outward like a tree, helping to satisfy the mean-field assumptions, at least on the local scale. More precisely, the clusters' tendency to branch outward instead of curling in on themselves increases their overlap parameter, which suppresses the Ginsburg criterion, ϵ_G. It is only within ϵ_G of x_{perc} that the mean-field model breaks down and yields to critical percolation theory.[26] So, due to the monomers' stiffness, the mean-field approach is only expected to fail in a very narrow range of compositions. The second part of the explanation concerns the

https://doi.org/10.1021/acsmacrolett.4c00523
ACS Macro Lett. 2024, 13, 1545−1550

nature of the data presented here. While many researchers choose to zoom in on the percolation threshold and take measurements very close to x_{perc}, we focus instead on broad trends across a large composition range. Therefore, our data are not particularly sensitive to small deviations within the narrow range of compositions described above. This was not simply an oversight—the choice to survey a broad range of compositions was intentional, and is motivated by the practical needs of researchers designing CANs. When designing CANs for reprocessability, a theory that predicts network topology across the full range of experimentally accessible compositions is often more valuable than one that covers only a narrow region. For this reason, we conclude that the mean-field approach is the best candidate to describe the network topology of this model system, despite its simplifying assumptions.

More generally, we are optimistic that the mean-field approach will prove useful for many other mixed-composition CANs as well, particularly for similar high-T_g systems whose stiff monomers hinder the formation of small loops. In these systems especially, the theory's known inaccuracies are small, and confined to a narrow range of compositions. Overall, mean-field percolation theory appears well suited to describe broad trends across compositions in CANs, and provides valuable insight into network topology both above and below the percolation threshold. As interest in CANs continues to grow, with more and more new systems under development, understanding network topology will be key to effectively design for reprocessability.

■ ASSOCIATED CONTENT

Data Availability Statement

Python scripts and raw data for generating figures in the main body of the paper and the supporting info are available at https://materialsdatafacility.org, findable by searching the title of this paper.

Supporting Information

The Supporting Information is available free of charge at https://pubs.acs.org/doi/10.1021/acsmacrolett.4c00523.

Time-lapse video of creep experiment (MP4)

Description of materials used, derivation and extensions of the mean-field model for CANs, discussion of molecular dynamics simulations, and mass spectra (PDF)

■ AUTHOR INFORMATION

Corresponding Author

Kenneth R. Shull − *Department of Materials Science and Engineering, Northwestern University, Evanston, Illinois 60208, United States;* orcid.org/0000-0002-8027-900X; Email: k-shull@northwestern.edu

Authors

Benjamin R. Hafner − *Department of Materials Science and Engineering, Northwestern University, Evanston, Illinois 60208, United States;* orcid.org/0009-0005-4140-2692

Subhadeep Pal − *Department of Civil and Environmental Engineering, Northwestern University, Evanston, Illinois 60208, United States;* orcid.org/0000-0002-0532-9791

Broderick Lewis − *Department of Materials Science and Engineering, Northwestern University, Evanston, Illinois 60208, United States;* orcid.org/0009-0009-4607-7939

Sinan Keten − *Department of Mechanical Engineering and Department of Civil and Environmental Engineering, Northwestern University, Evanston, Illinois 60208, United States*

Complete contact information is available at: https://pubs.acs.org/10.1021/acsmacrolett.4c00523

Author Contributions

CRediT: **Benjamin R Hafner** conceptualization, data curation, formal analysis, investigation, methodology, software, visualization, writing - original draft, writing - review & editing; **Subhadeep Pal** data curation, investigation, methodology, software, writing - review & editing; **Broderick Lewis** methodology, supervision, writing - review & editing; **Sinan Keten** funding acquisition, writing - review & editing; **Kenneth R Shull** funding acquisition, supervision, writing - review & editing.

Notes

The authors declare no competing financial interest.

■ ACKNOWLEDGMENTS

This material is based upon work supported by the National Science Foundation under Grants No. DMR-2308601 and OISE-1743748. B.R.H. acknowledges support from a Paglia Post-Baccalaureate Research Fellowship from Carleton College. The work made use of the Integrated Molecular Structure Education and Research Center (IMSERC) at Northwestern University, which has received support from the Soft and Hybrid Nanotechnology Experimental (SHyNE) Resource (NSF ECCS-1542205), the State of Illinois, and the International Institute for Nanotechnology (IIN). This work also made use of the CLaMMP Facility which has received support from the MRSEC Program (DMR-2308691) of the Materials Research Center at Northwestern University, the Center for Hierarchical Materials Design and from Northwestern University.

■ REFERENCES

(1) Kloxin, C. J.; Bowman, C. N. Covalent adaptable networks: smart, reconfigurable and responsive network systems. *Chem. Soc. Rev.* **2013**, *42*, 7161−7173.

(2) Cash, J. J.; Kubo, T.; Dobbins, D. J.; Sumerlin, B. S. Maximizing the symbiosis of static and dynamic bonds in self-healing boronic ester networks. *Polym. Chem.* **2018**, *9*, 2011−2020.

(3) Li, L.; Chen, X.; Jin, K.; Torkelson, J. M. Vitrimers designed both to strongly suppress creep and to recover original cross-link density after reprocessing: Quantitative theory and experiments. *Macromolecules* **2018**, *51*, 5537−5546.

(4) Konuray, O.; Moradi, S.; Roig, A.; Fernández-Francos, X.; Ramis, X. Thiol−Ene Networks with Tunable Dynamicity for Covalent Adaptation. *ACS Applied Polymer Materials* **2023**, *5*, 1651−1656.

(5) Flory, P. J. Molecular size distribution in three dimensional polymers. I. Gelation1. *Journal of the American chemical society* **1941**, *63*, 3083−3090.

(6) Flory, P. J. Molecular size distribution in three dimensional polymers. II. Trifunctional branching units. *J. Am. Chem. Soc.* **1941**, *63*, 3091−3096.

(7) Stockmayer, W. H. Theory of molecular size distribution and gel formation in branched-chain polymers. *J. Chem. Phys.* **1943**, *11*, 45−55.

(8) Macosko, C. W.; Miller, D. R. A new derivation of average molecular weights of nonlinear polymers. *Macromolecules* **1976**, *9*, 199−206.

(9) Miller, D. R.; Macosko, C. W. A new derivation of postgel properties of network polymers. *Rubber chemistry and technology* **1976**, *49*, 1219−1231.

(10) Chen, L.; Zhang, L.; Griffin, P. J.; Rowan, S. J. Impact of Dynamic Bond Concentration on the Viscoelastic and Mechanical Properties of Dynamic Poly (alkylurea-co-urethane) Networks. *Macromol. Chem. Phys.* **2020**, *221*, 1900440.
(11) Moradi, S.; Fernández-Francos, X.; Konuray, O.; Ramis, X. Recyclable dual-curing thiol-isocyanate-epoxy vitrimers with sequential relaxation profiles. *Eur. Polym. J.* **2023**, *196*, 112290.
(12) Stauffer, D.; Coniglio, A.; Adam, M. *Polymer networks*; Springer: 2005; pp 103−158.
(13) Nevejans, S.; Ballard, N.; Miranda, J. I.; Reck, B.; Asua, J. M. The underlying mechanisms for self-healing of poly (disulfide) s. *Phys. Chem. Chem. Phys.* **2016**, *18*, 27577−27583.
(14) Matxain, J. M.; Asua, J. M.; Ruipérez, F. Design of new disulfide-based organic compounds for the improvement of self-healing materials. *Phys. Chem. Chem. Phys.* **2016**, *18*, 1758−1770.
(15) Ruiz de Luzuriaga, A.; Martin, R.; Markaide, N.; Rekondo, A.; Cabanero, G.; Rodriguez, J.; Odriozola, I. Epoxy resin with exchangeable disulfide crosslinks to obtain reprocessable, repairable and recyclable fiber-reinforced thermoset composites. *Materials Horizons* **2016**, *3*, 241−247.
(16) Lewis, B.; Dennis, J. M.; Shull, K. R. Effects of Dynamic Disulfide Bonds on Mechanical Behavior in Glassy Epoxy Thermosets. *ACS Applied Polymer Materials* **2023**, *5*, 2583−2595.
(17) Ruiz de Luzuriaga, A.; Matxain, J. M.; Ruiperez, F.; Martin, R.; Asua, J. M.; Cabanero, G.; Odriozola, I. Transient mechanochromism in epoxy vitrimer composites containing aromatic disulfide crosslinks. *Journal of Materials Chemistry C* **2016**, *4*, 6220−6223.
(18) Lewis, B.; Dennis, J. M.; Park, C.; Shull, K. R. Glassy Dynamics of Epoxy-Amine Thermosets Containing Dynamic, Aromatic Disulfides. *Macromolecules* **2024**, *57*, 7112−7122.
(19) Takahashi, A.; Ohishi, T.; Goseki, R.; Otsuka, H. Degradable epoxy resins prepared from diepoxide monomer with dynamic covalent disulfide linkage. *Polymer* **2016**, *82*, 319−326.
(20) Tesoro, G.; Sastri, V. Reversible crosslinking in epoxy resins. I. Feasibility studies. *J. Appl. Polym. Sci.* **1990**, *39*, 1425−1437.
(21) Pal, S.; Dansuk, K.; Giuntoli, A.; Sirk, T. W.; Keten, S. Predicting the Effect of Hardener Composition on the Mechanical and Fracture Properties of Epoxy Resins Using Molecular Modeling. *Macromolecules* **2023**, *56*, 4447.
(22) Giuntoli, A.; Hansoge, N. K.; van Beek, A.; Meng, Z.; Chen, W.; Keten, S. Systematic coarse-graining of epoxy resins with machine learning-informed energy renormalization. *npj Comput Mater* **2021**, *7*, 168.
(23) Abbott, L. J.; Hart, K. E.; Colina, C. M. Polymatic: a generalized simulated polymerization algorithm for amorphous polymers. *Theor Chem Acc* **2013**, *132*, 1334.
(24) Xu, X.; Wang, J.; Lv, J.-P.; Deng, Y. Simultaneous analysis of three-dimensional percolation models. *Front. Phys.* **2014**, *9*, 113−119.
(25) Si, H.; Zhou, L.; Wu, Y.; Song, L.; Kang, M.; Zhao, X.; Chen, M. Rapidly reprocessable, degradable epoxy vitrimer and recyclable carbon fiber reinforced thermoset composites relied on high contents of exchangeable aromatic disulfide crosslinks. *Composites Part B: Engineering* **2020**, *199*, 108278.
(26) Rubinstein, M.; Colby, R. H. *Polymer physics*; Oxford University Press: 2003.

https://doi.org/10.1021/acsmacrolett.4c00523
ACS Macro Lett. 2024, 13, 1545−1550